Mixed-Mode, High-Cycle Fatigue-Crack Growth Thresholds in Ti-6Al-4V: A Comparison of Large and Small Crack Behavior[1]

R. K. Nalla, J. P. Campbell and R. O. Ritchie[2]

Department of Materials Science and Engineering
University of California, Berkeley, CA 94720-1760

ABSTRACT: *There are few experimental results to date describing the crack-propagation threshold behavior of short fatigue cracks under multiaxial loading conditions. To address this need, in the present study, the variation in mixed-mode, high-cycle fatigue-crack growth thresholds with crack size and shape are reported for a Ti-6Al-4V turbine blade alloy, heat treated to two widely different microstructural conditions, namely fine-grained bimodal and coarser fully lamellar microstructures. Specifically, fatigue thresholds are examined for through-thickness large cracks (as compared to the microstructural dimensions), through-thickness short cracks (< 200 µm in length), and small, semi-elliptical surface cracks (comparable with microstructural dimensions), under the effect of combined mode I and mode II loading for load ratios (ratio of minimum to maximum load) ranging from 0.1 to 0.8. For a range of mode-mixities, large crack, mode I thresholds, $\Delta K_{I,TH}$, were found to be decrease substantially with increasing phase angle. However, by characterizing in terms of the range in strain energy release rate, ΔG_{TH}, incorporating both mode I and mode II contributions, it was observed that the pure mode I threshold could be regarded as a "worst case" large crack threshold under mixed-mode loading in this alloy. An estimation of the shielding-corrected, crack-driving forces actually experienced at the crack tip was also performed. For such near-tip (shielding-corrected) thresholds, the influence of mode-mixity was dramatically reduced. Corresponding thresholds for through-thickness short cracks and small surface cracks, where the effect of such shielding is minimized, were also substantially less sensitive to mode-mixity and corresponded in magnitude to the shielding-corrected large crack thresholds.*

INTRODUCTION

The occurrence and control of failure due to high cycle fatigue (HCF) in turbine engine components is currently one of the most critical challenges facing the U.S. military aircraft fleet. One particular challenge is the prediction of

[2]*contributing author:* Prof. R. O. Ritchie
Department of Materials Science and Engineering
463 Evans Hall, #1760, University of California, Berkeley, CA 94720-1760
tel: +1 (510) 486-5798; fax: +1 (510) 486-4882; e-mail: RORitchie@lbl.gov

the limiting conditions for failure in the presence of multiaxial stresses, which can occur, for example, in association with fretting fatigue in the blade dovetail/disk contact section [1]. Although the driving force for these situations is a combination of tensile (mode I), in-plane shear (mode II) and anti-plane shear (mode III) loading, most studies of the fatigue-crack growth behavior of typical turbine blade alloys, such as Ti-6Al-4V, have been focused on pure mode I behavior [2-6]. Indeed, only a few investigations have examined the role of increasing mode-mixity on the variation in fatigue thresholds in such alloys [7-11].

Based on this work, the superposition of shear (with corresponding finite stress-intensity ranges in mode II, ΔK_{II}, or mode III, ΔK_{III},) was shown to cause a substantial reduction in the mode I fatigue threshold, $\Delta K_{I,TH}$ [9,11]. Studies, however, were concentrated on large-crack behavior; corresponding research on the mixed-mode threshold behavior of small cracks is essentially non-existent. This is particularly troubling for the HCF problem as the variation in threshold behavior with mode-mixity is known to depend critically on the degree of crack-tip shielding (by mode I crack closure and mode II crack surface interference [9-11,12]), which serves to locally reduce the effective driving force at the tip [e.g., 10], and it is widely known that the potency of such shielding is substantially reduced for small cracks with limited wake.

Accordingly, the role of crack size is examined in the present work through a study of the mixed-mode, long and short crack fatigue crack growth thresholds in a Ti-6Al-4V alloy with bimodal and fully lamellar microstructures. Experiments were performed for mode-mixities varying from pure tension ($\Delta K_{II} / \Delta K_I = 0$) to predominantly shear ($\Delta K_{II} / \Delta K_I \sim 7.1$), over a range of load ratios (minimum load/maximum load) from $R = 0.1$ to 0.8.

EXPERIMENTAL PROCEDURES

The material investigated was a turbine engine alloy Ti-6Al-4V, with composition (in wt.%) 6.3Al, 4.17V, 0.19Fe, 0.19O, 013N, 0.0041H, bal. Ti. The alloy was examined with microstructures: (i) the as-received, bimodal condition (sometimes referred to as solution treated and overaged - STOA), consisting of colonies of ~60% equiaxed primary α (average grain size 20 µm) within ~40% lamellar $\alpha+\beta$ (Fig. 1(a)), and (ii) a fully lamellar structure

obtained by heat treating at 1010^oC for 10 min, rapid quenching in helium and stabilizing for 2 hr at 700^oC, to give an average colony size of 500 μm (Fig. 1(b)). Full processing details are given elsewhere [13]. Strength levels were found to be 930 MPa (yield) and 978 MPa (UTS) in the bimodal structure and 975 MPa (yield) and 1055 MPa (UTS) in the lamellar structure.
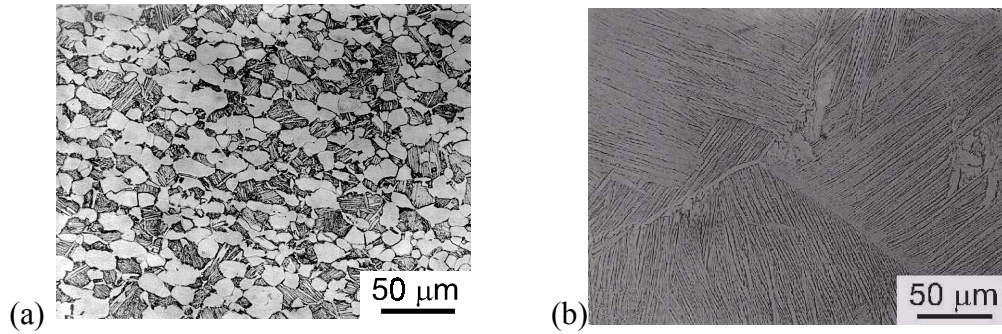

(a)　　　　　　　　　　　　　　　　　(b)

Figure 1: Optical micrographs of (a) bimodal and (b) lamellar microstructures. Etched ~10 s in 5 parts 70% HNO_3, 10 parts 50% HF, 85 parts of H_2O.

Precracking was conducted in room air in near-identical manner for all long-crack test samples. Specifically, fatigue cracks were grown from a 2 mm deep electro-deposition machined notch in a symmetric four-point bending sample at a load ratio of 0.1 with a loading frequency of 50 Hz. (This alloy shows little effect of frequency in air over the range 50 to 20,000 Hz [14]). The final precrack length was 4.50 ± 0.25 mm at a final near-threshold ΔK of, respectively, 4.8 ± 0.5 and 6.8 ± 0.5 MPa$\sqrt{m}$ in bimodal and lamellar specimens.

Pure mode I tests were conducted using symmetric four-point bending with inner and outer spans of 12.7 and 25.4 mm respectively. For mixed-mode loading, the mode II component of the loading was introduced using the asymmetric four-point bending configuration, where the $\Delta K_{II}/\Delta K_I$ ratio can be varied using an offset from the load-line shown in Fig. 2 [e.g., ref. 15]. The values of ΔK_I and ΔK_{II} were determined from linear elastic stress intensity solutions for this geometry, recently developed by He and Hutchinson [16].
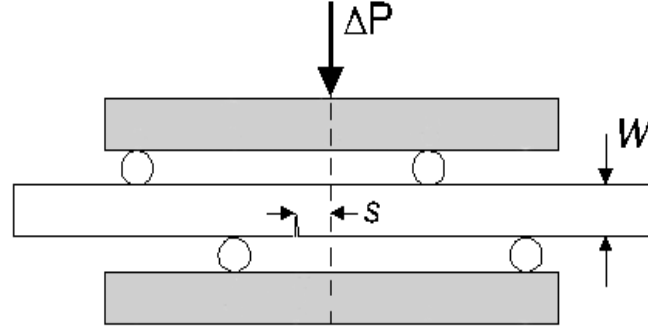
Figure 2: The asymmetric four-point bend specimen. The offset *s*, from the load-line is used to control the degree of mode-mixity ($\Delta K_{II} / \Delta K_I$).

For long-crack (>4 mm) tests, mode-mixities varied from $\Delta K_{II}/\Delta K_I$ = 0 to 7.1, representing a change in phase angle, $\beta = \tan^{-1}(\Delta K_{II} / \Delta K_I)$, from $0°$ to $82°$. Load ratios were varied from R = 0.1 to 0.8. Tests involving cycling pre-cracked specimens at a specified mode-mixity were performed in the following way; if no crack growth was observed (using an optical microscope) after a given number of cycles (2 x 10^6 in the bimodal and 5 x 10^6 in the lamellar structure), either ΔK_I or ΔK_{II} was increased by ~0.25 MPa$\sqrt{m}$ and the procedure repeated. In this way, a "growth/no growth" condition bounding the threshold was obtained. The crack extension defining "growth" was taken to be of the order of the characteristic microstructural dimension, i.e., ~20 and 500 μm for the bimodal and lamellar microstructures, respectively.

For corresponding tests on short cracks, thresholds were measured using identical procedures, except that the precrack wake was the carefully machined to within ~200 μm of the crack tip using a slow-speed diamond saw.

RESULTS AND DISCUSSION

Mixed-Mode Long Crack Threshold Envelopes

Mixed-mode threshold envelopes for long cracks, with the mode II threshold stress-intensity range, $\Delta K_{II,TH}$, plotted as a function of the corresponding mode I threshold, $\Delta K_{I,TH,}$ are shown in Fig. 3 for both structures. A clear reduction in

threshold values with increasing R is evident, as shown by the inward shift of the threshold envelopes.
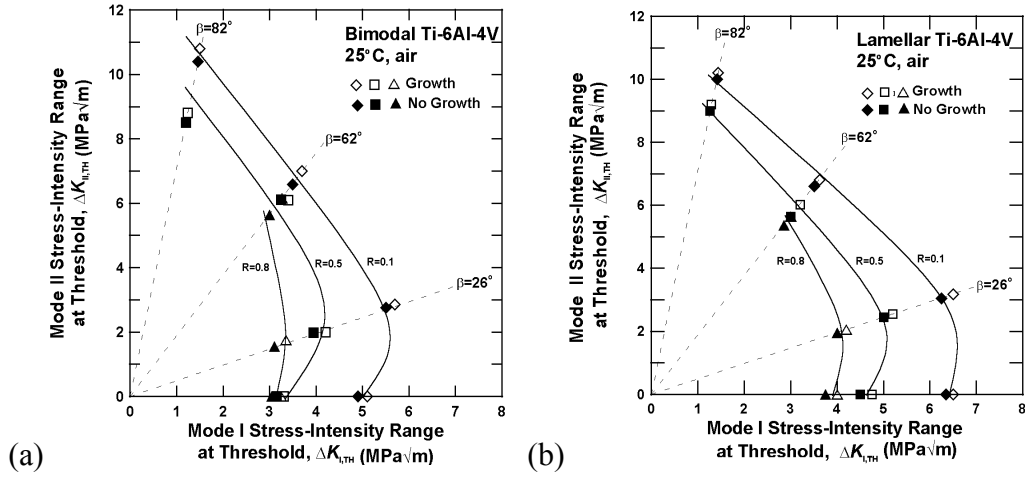

Figure 3: Mixed-mode threshold envelopes for (a) bimodal and (b) fully lamellar microstructures. Note that the lamellar structure shows superior resistance to crack propagation, particularly at the lower phase angles.

In general, the lamellar microstructure showed a better resistance to long-crack growth, which can be attributed to an enhanced influence of crack-tip shielding induced by the coarser microstructure, as discussed in detail elsewhere [11]. The effect of microstructure, however, is reduced considerably at high mode-mixities.

Single Parameter Characterization

Although the mode I threshold, $\Delta K_{I,TH}$, decreases with increasing mode-mixity, a more appropriate measure of the mixed-mode driving force is the range in strain-energy release rate, $\Delta G = (\Delta K_I^2 + \Delta K_{II}^2) / E$, where $E = E$ (Young's modulus) in plane stress and $E / (1-v^2)$ in plane strain (v is Poisson's ratio). As shown in Fig. 4, when used to characterize the mixed-mode fatigue threshold behavior as a function of the phase angle β, there is a progressive increase in the mixed-mode threshold, ΔG_{TH}, with increasing mode-mixity in both

microstructures for all load ratios studied. Indeed, it is clear that the mode I threshold, defined in terms of ΔG, represents a *worst-case* condition.

Comparison of Thresholds for Short and (Shielding-Corrected) Long Cracks

The short crack threshold data are also presented in Fig. 4 along with a scatter band of *shielding-corrected* long crack threshold results (Fig. 4). The shielding-correction was based on compliance-based measurements of the mode I crack closure and mode II crack-surface interference, as described elsewhere [10].

Short crack thresholds were observed within the scatter band for shielding-corrected long cracks, indicating that as for mode I conditions, the limited effect of shielding for short cracks is responsible for their lower threshold values. More importantly, the marked influence of mode-mixity in increasing mixed-mode thresholds for long cracks is largely absent in the short-crack results, again implying the prominent role of crack-tip shielding (particularly shear-induced) in causing the mode-mixity effect on long-crack thresholds. As the thresholds for short cracks are considerably lower, and far less influenced by mode-mixity, than those for long cracks, it is clear that the use of mixed-mode
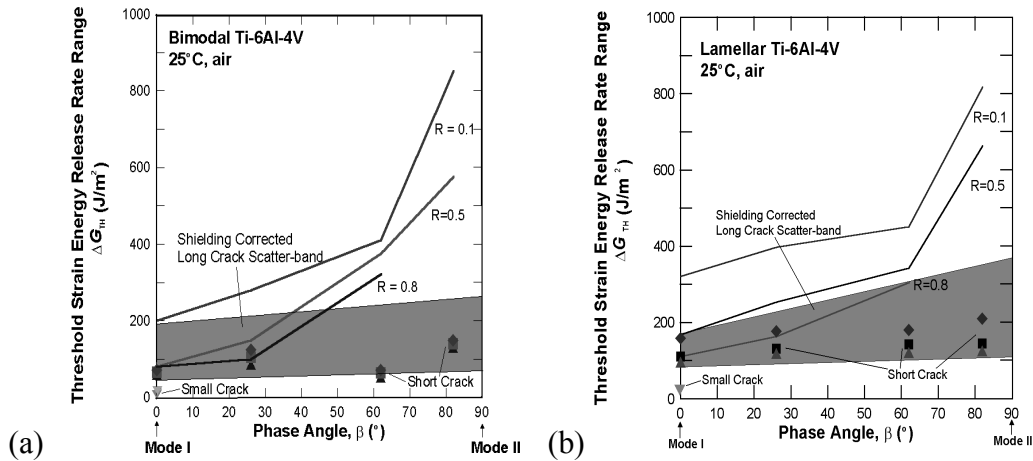

Figure 4: Variation in mixed-mode threshold, ΔG_{TH}, as a function of phase angle, β, in (a) bimodal and (b) lamellar structures. Shown are results at three load ratios for long (> 4 mm) cracks, before and after "correcting" for crack-tip shielding, and short (~200 μm) cracks. Also plotted are the mode I thresholds for small (~10 μm) surface cracks.

threshold data in the literature, which is almost exclusively for large flaws, may be highly non-conservative.

Mixed-Mode Small Crack Growth Studies

The results presented show a marked effect of crack size on the mixed-mode thresholds. However, the short cracks examined were still of a size large compared to microstructural dimensions, particularly in the bimodal alloy. Mixed-mode results for microstructurally small cracks are currently under investigation. However, mode I thresholds for such cracks, in this instance ~10 µm in surface length, are shown in Fig. 4, and display even lower threshold values in both microstructures. In fact, the long crack ΔG_{TH} threshold in the bimodal alloy at $\Delta K_{II}/\Delta K_I = 7.1$ at $R = 0.1$ is some 90 times larger than this small crack threshold. Since there is little to no information in the literature concerning the mixed-mode behavior of such small flaws, this is clearly an important topic for future investigation.

CONCLUSIONS

Mixed-mode (mode I + II) fatigue crack growth thresholds for long (> 4 mm) and short (~200 µm) cracks have been examined in bimodal and fully lamellar microstructures in a Ti-6Al-4V alloy in symmetric and asymmetric four-point bend samples over a range of mode-mixities from $\Delta K_{II}/\Delta K_I = 0$ to 7.1 at load ratios between 0.1 and 0.8.

The large influence of increasing mode-mixity on the mixed-mode fatigue threshold ΔG_{TH}, observed for long cracks at load ratios between 0.1 and 0.8, was found to be substantially diminished for short cracks. Moreover, the magnitude of such short crack thresholds was significantly lower than those measured for long cracks; indeed their values were found to be comparable with the crack-tip shielding-corrected long crack thresholds, which suggests a prominent role of shielding on long crack mixed-mode behavior. Although data are essentially non-existent, this marked reduction in ΔG_{TH} thresholds may be even larger for microstructurally-small cracks. Finally, the present results indicate that the ΔG_{TH} thresholds in pure mode I in the Ti-6Al-4V alloy can be taken as the *worst case* in both long and short crack regimes.

REFERENCES

1. Cowles, B. A. (1996) *Int. J. Fracture* **80**, pp. 147-163.
2. Ritchie, R. O., Boyce, B. L., Campbell, J. P., Roder, O., Thompson, A. W., and Milligan, W. W. (1999) *Int. J. Fatigue* **21**, pp. 653-662.
3. Ravichandran, K. S. (1991) *Acta Metall. Mater.* **39**, pp. 401-410.
4. Thompson, A. W. (1999), In: *Fatigue Behavior of Titanium Alloys*, pp. 23-30, Boyer, R.R., Eylon, D., and Lütjering, G. (Eds.), TMS, Warrendale, PA.
5. Gregory, J. K. (1994) In: *Handbook of Fatigue Crack Propagation in Metallic Structures*, pp. 281-321, Carpinteri, A. (Ed.), Elsevier, London.
6. Lütjering, G. (1998) *Mater. Sci. Eng.* **A263**, pp. 117-126.
7. Gao, H., Alagok, N., Brown, M. W., and Miller, K. J. (1985) In: *Multiaxial Fatigue*, pp. 184-205, Miller, K. J. and Brown, M.W. (Eds.), ASTM STP 853. American Society for Testing and Materials., Philadelphia.
8. Pustejovsky, M. A. (1979) *Eng. Fract. Mech*. **11**, pp. 9-31.
9. Campbell, J. P. and Ritchie, R. O. (2000) *Eng. Fract. Mech.* **67**, pp. 209-227.
10. Campbell, J. P. and Ritchie, R. O. (2000) *Eng. Fract. Mech.* **67**, pp. 229-249.
11. Campbell, J. P. and Ritchie, R. O. (2001) *Metall. Mater. Trans. A* **31A**.
12. Tong, J., Yates, J. R., and Brown, M. W. (1995) *Eng. Fract. Mech*. **52**, pp. 599-623.
13. Eylon, D. (1998) Summary of Available Information on the Processing of the Ti-6Al-4V HCF/LCF Program Plates, Univ. Dayton Rep., Dayton, OH.
14. Ritchie, R. O., Davidson, D. L., Boyce, B. L., Campbell, J. P., and Roder, O. (1999) *Fat. Fract. Eng. Mat. Struct*. **22**, pp. 621-631.
15. Suresh, S., Shih, C. F., Morrone, A., and O'Dowd, N. P. (1990) *J. Am. Ceram. Soc.* **73**, pp. 1257-1267.
16. He, M. Y. and Hutchinson, J. W. (2000) *J. Appl. Mech.* **67**, pp. 207-209.